O.M. VOLKOV,[1] V.P. KRAVCHUK [2]

[1] Taras Shevchenko National University of Kyiv
(64, Volodymyrs'ka Str., Kyiv 01601, Ukraine; e-mail: alexey@volkov.ca)
[2] Bogolyubov Institute for Theoretical Physics, Nat. Acad. of Sci. of Ukraine
(14-b, Metrolohichna Str., Kyiv 03680, Ukraine; e-mail: vkravchuk@bitp.kiev.ua)

SATURATION OF MAGNETIC FILMS WITH SPIN-POLARIZED CURRENT IN THE PRESENCE OF A MAGNETIC FIELD

PACS 75.10.Hk, 75.40.Mg, 05.45.-a, 72.25.Ba, 85.75.-d

The influence of a perpendicular magnetic field on the process of transversal saturation of ferromagnetic films with spin-polarized current is studied theoretically. It is shown that the saturation current J_s is decreased (increased) in the case of the codirected (oppositely directed) magnetic field and the current. There exists a critical current $J_c > J_s$, which provides a "rigid" saturation – the saturated state is stable with respect to the transverse magnetic field of any amplitude and direction. The influence of a magnetic field on the vortex-antivortex crystals, which appear in a pre-saturated regime, is studied numerically. All analytical results are verified using micromagnetic simulations.

K e y w o r d s: spin-polarized current, magnetic films, magnetic field.

1. Introduction

The influence of a spin-polarized current on planar magnetic systems is of high applied and academic interest now. It is so mainly due to the possibility to handle the magnetization states of magnetic nanoparticles (nanomagnets) without using the external magnetic fields of complex space-time configurations. That provides new opportunities in the construction of purely current controlled devices [1], e.g., magnetic disk drivers or Magnetic Random Access Memory (MRAM) [2, 3].

A convenient way to provide the influence of a spin-polarized current on the magnetic film is to use a pillar structure which was firstly proposed in Ref. [4]. The simplest pillar structure consists of two ferromagnetic layers (polarizer and sample) and nonmagnetic spacer between them, see Fig. 1. When the electrical current passes through the polarizer, the conduction electrons become partially spin-polarized in the direction that is determined by the polarizer magnetization. The polarizer is usually made of a hard ferromagnetic material, whose magnetization is kept fixed. The spacer, being very thin (few nanometers), does not change the spin polarization of the current electrons, but it prevents the exchange interaction between the polarizer and the sample. Thus, the spin-polarized electrons transfer the spin-torque from the polarizer to the sample, which can result in the dynamics of the sample magnetization. The spin-torque influence can be described phenomenologically by adding the Slonczewski–Berger term to the Landau–Lifshitz equation [5–7].

Recently, we studied the influence of a strong spin-current on the magnetic films [8, 9]. It was shown that the strong spin-polarized current can saturate the magnetic film, and the value of saturation current density J_s increases with the film thickness. We also demonstrated that, in the pre-saturated regime, stable vortex-antivortex lattices (VAL) appear. As was recently shown [10, 11], the external magnetic field can drastically modify magnetic system's dynamics induced by the spin-torque. The aim of this paper is to study the influence of a perpendicular magnetic

field on the process of film saturation with the spin-current. For this purpose, we modify the linear theory of instability of the saturated state developed in Ref. [9] to the case of the presence of a magnetic field and a uniaxial anisotropy. This will enable us to obtain the dependence of the saturation current J_s on the field amplitude. We will demonstrate that, in the linear approximation, the actions of a perpendicular magnetic field and a uniaxial anisotropy on the stability of the saturated state are equivalent. Using micromagnetic simulations, we study how the properties of the VAL, which appear it the pre-saturated regime, depend on the value of the applied field.

2. Theory of Saturated State Stability

Let us consider a ferromagnetic film with thickness h and lateral size $L \gg h$. We use a discrete model of magnetic media considering a three-dimensional cubic lattice of magnetic moments $\mathbf{M}_{\boldsymbol{\nu}}$ with lattice spacing $a \ll h$, where $\boldsymbol{\nu} = a(\nu_x, \nu_y, \nu_z)$ is a three-dimensional index with $\nu_x, \nu_y, \nu_z \in \mathbb{Z}$ (here and below, all Greek indices are three-dimensional and the Latin indices are two-dimensional). We assume also that h is small enough to ensure the magnetization uniformity along the thickness. In this case, one can use the two-dimensional discrete Landau–Lifshitz–Slonczewski equation [5–7],

$$\dot{\mathbf{m}}_{\mathbf{n}} = \mathbf{m}_{\mathbf{n}} \times \frac{\partial \mathcal{E}}{\partial \mathbf{m}_{\mathbf{n}}} - \varkappa \frac{\mathbf{m}_{\mathbf{n}} \times [\mathbf{m}_{\mathbf{n}} \times \hat{\mathbf{z}}]}{1 + (\mathbf{m}_{\mathbf{n}} \cdot \hat{\mathbf{z}})}, \tag{1}$$

to describe the magnetization dynamics under the influence of a spin-polarized current, which flows perpendicularly to the magnetic plane along the $\hat{\mathbf{z}}$-axis (see Fig. 1). It is also assumed that the current flow and its spin-polarization are of the same direction in Eq. (1). The two-dimensional index $\mathbf{n} = a(n_x, n_y)$ with $n_x, n_y \in \mathbb{Z}$ enumerates the normalized magnetic moments $\mathbf{m}_{\mathbf{n}} = \mathbf{M}_{\mathbf{n}}/|\mathbf{M}_{\mathbf{n}}|$ within the film plane. The overdot indicates the derivative with respect to the rescaled time in units of $(4\pi\gamma M_s)^{-1}$, γ is the gyromagnetic ratio, M_s is the saturation magnetization, and $\mathcal{E} = E/(4\pi M_s^2 a^3 \mathcal{N}_z)$ is the dimensionless magnetic energy, where $\mathcal{N}_z = h/a$ is the number of magnetic moments along the thickness. The normalized current density is presented by the parameter $\varkappa = \eta J/J_0$, where η is the degree of spin polarization, J is the current density, and $J_0 = 4\pi M_s^2 |e| h/\hbar$ with e being the electron charge, and $\hbar$ being Planck's constant.

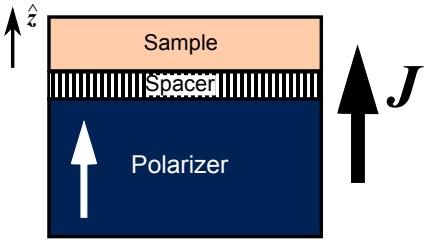

Fig. 1. The simplest pillar heterostructure consists of two ferromagnetic layers: the polarizer and the sample, and one nonmagnetic layer between them (spacer). Black (larger) arrow shows the direction of a current, which flow through the heterostructure, and the white (smaller) arrow shows the magnetization direction of the polarizer

Equation (1) is written for the case where the conductance of the sample is much lower than the conductance of the spacer, which corresponds to a high level of spin accumulation at the nonmagnet–ferromagnet interfaces. The mismatch between the spacer and ferromagnet resistances is traditionally described by the Λ-parameter [7, 12]. But as was shown in Ref. [9], the parameter Λ is not included in the linearized problem and, therefore, has no influence on the saturation process. That is why we do not include Λ into our model assuming $\Lambda \gg 1$. We also omitted a damping in the equation of motion (1), because, as was shown earlier [9], the spin-current provides an effective damping which is much larger than the natural damping.

We consider a magnetic system, the total energy $E = E_{\text{ex}} + E_{\text{d}} + E_{\text{z}} + E_{\text{an}}$ of which consists of four parts: exchange, dipole-dipole, Zeeman, and magnetocrystalline anisotropy contributions. The exchange energy up to a constant has the form

$$E_{\text{ex}} = -\mathcal{S}^2 \mathcal{N}_z \mathcal{J}_0 \sum_{\mathbf{n},\tilde{\mathbf{n}}} \mathbf{m}_{\mathbf{n}} \cdot \mathbf{m}_{\mathbf{n}+\tilde{\mathbf{n}}}, \tag{2}$$

where $\tilde{\mathbf{n}}$ enumerates the nearest neighbors within the film plane of the $\mathbf{n}$-th atom, $\mathcal{S}$ is the value of spin of a ferromagnetic atom, and $\mathcal{J}_0 > 0$ denotes the exchange integral between the nearest atoms.

The energy of dipole-dipole interaction is

$$E_{\text{d}} = \frac{M_s^2 a^6}{2} \times$$

$$\times \sum_{\boldsymbol{\nu} \neq \boldsymbol{\lambda}} \left[\frac{(\mathbf{m}_{\boldsymbol{\nu}} \cdot \mathbf{m}_{\boldsymbol{\lambda}})}{r_{\boldsymbol{\lambda}\boldsymbol{\nu}}^3} - 3 \frac{(\mathbf{m}_{\boldsymbol{\nu}} \cdot \mathbf{r}_{\boldsymbol{\lambda}\boldsymbol{\nu}})\,(\mathbf{m}_{\boldsymbol{\lambda}} \cdot \mathbf{r}_{\boldsymbol{\lambda}\boldsymbol{\nu}})}{r_{\boldsymbol{\lambda}\boldsymbol{\nu}}^5} \right], \tag{3}$$

where $\mathbf{r}_{\boldsymbol{\lambda\nu}} = \boldsymbol{\lambda} - \boldsymbol{\nu}$, with $\boldsymbol{\lambda}$ and $\boldsymbol{\nu}$ being the three-dimensional indices.

The Zeeman energy describes the interaction of the magnetic film with the external perpendicular magnetic field $\mathbf{B} = B\hat{\mathbf{z}}$, and it reads

$$E_{\rm z} = -BM_s a^3 \mathcal{N}_z \sum_{\mathbf{n}} m^z_{\mathbf{n}}. \tag{4}$$

Finally, we introduce the energy of uniaxial anisotropy, whose axis is oriented perpendicularly to the film plane:

$$E_{\rm an} = -\frac{K}{2} a^3 \mathcal{N}_z \sum_{\mathbf{n}} (m^z_{\mathbf{n}})^2, \tag{5}$$

where K is the anisotropy coefficient, which can be positive (easy-axis) or negative (easy-plane).

By introducing the complex variable [9]

$$\psi_{\mathbf{n}} = \frac{m^x_{\mathbf{n}} + i m^y_{\mathbf{n}}}{\sqrt{1 + m^z_{\mathbf{n}}}}, \tag{6}$$

we can write Eq. (1) in the form

$$i\dot{\psi}_{\mathbf{n}} = -\frac{\partial \mathcal{E}}{\partial \psi^*_{\mathbf{n}}} - i\frac{\partial \mathcal{F}}{\partial \psi^*_{\mathbf{n}}}, \tag{7}$$

where the function

$$\mathcal{F} = \frac{\varkappa}{2} \sum_{\mathbf{n}} |\psi_{\mathbf{n}}|^2 \tag{8}$$

represents an action of the spin-polarized current.

For the future analysis, it is convenient to pass to the wave-vector representation, using the two-dimensional discrete Fourier transformation:

$$\psi_{\mathbf{n}} = \frac{1}{\sqrt{\mathcal{N}_{xy}}} \sum_{\mathbf{k}} \hat{\psi}_{\mathbf{k}} e^{i\mathbf{k}\cdot\mathbf{n}}, \tag{9a}$$

$$\hat{\psi}_{\mathbf{k}} = \frac{1}{\sqrt{\mathcal{N}_{xy}}} \sum_{\mathbf{n}} \psi_{\mathbf{n}} e^{-i\mathbf{k}\cdot\mathbf{n}} \tag{9b}$$

with the orthogonality condition

$$\sum_{\mathbf{n}} e^{i(\mathbf{k}-\mathbf{k}')\cdot\mathbf{n}} = \mathcal{N}_{xy} \Delta(\mathbf{k} - \mathbf{k}'), \tag{10}$$

where $\mathcal{N}_{xy} = L^2/a^2$ is the total number of atoms within the film plane, $\mathbf{k} = (k_x, k_y) \equiv \frac{2\pi}{L}(l_x, l_y)$ is the two-dimensional discrete wave vector, $l_x, l_y \in \mathbb{Z}$, and $\Delta(\mathbf{k})$ is the Kronecker delta.

Applying (9) to Eq. (7), we obtain the equation of motion in the reciprocal space:

$$-i\dot{\hat{\psi}}_{\mathbf{k}} = \frac{\partial \mathcal{E}}{\partial \hat{\psi}^*_{\mathbf{k}}} + i\frac{\partial \mathcal{F}}{\partial \hat{\psi}^*_{\mathbf{k}}}. \tag{11}$$

Since we are studying the stability of the saturated state, we can linearize the equation of motion (11) in a vicinity of the solution $m^z_{\mathbf{n}} = 1$, which is equivalent to $|\psi_{\mathbf{n}}| = 0$ and $|\hat{\psi}_{\mathbf{k}}| = 0$. To obtain the energy functional $\mathcal{E}$ in the "ψ"-representation, we expand components of the magnetization vector into series in the way similar to the representation in terms of the Bose operators [13]:

$$\begin{aligned} m^x_{\mathbf{n}} &= \frac{\psi_{\mathbf{n}} + \psi^*_{\mathbf{n}}}{\sqrt{2}} + \mathcal{O}(|\psi_{\mathbf{n}}|^3), \\ m^y_{\mathbf{n}} &= \frac{\psi_{\mathbf{n}} - \psi^*_{\mathbf{n}}}{i\sqrt{2}} + \mathcal{O}(|\psi_{\mathbf{n}}|^3), \\ m^z_{\mathbf{n}} &= 1 - |\psi_{\vec{n}}|^2. \end{aligned} \tag{12}$$

Substituting (12) into the energy components (2)–(5) and applying the Fourier transformation (9), (10), we can write the dimensionless energy functional in the form

$$\mathcal{E} = \mathcal{E}_{\rm ex} + \mathcal{E}_{\rm d} + \mathcal{E}_{\rm z} + \mathcal{E}_{\rm an}. \tag{13a}$$

Here, the exchange contribution reads [9]

$$\mathcal{E}_{\rm ex} = \ell^2 \sum_{\mathbf{k}} |\hat{\psi}_{\mathbf{k}}|^2 k^2 + \mathcal{O}(|\hat{\psi}_{\mathbf{k}}|^4), \tag{13b}$$

where $\ell = \sqrt{\mathcal{S}^2 \mathcal{J}_0 c/(4\pi M_s^2 a)}$ is the exchange length, with $c = 4$ being the number of nearest neighbors within the film plane. The energy of dipole-dipole interaction has the form [9]

$$\mathcal{E}_{\rm d} = \sum_{\mathbf{k}} \left[\frac{g(kh)}{2} - 1\right] |\hat{\psi}_{\mathbf{k}}|^2 +$$

$$+ \frac{g(kh)}{4} \left[\frac{(k^x - ik^y)^2}{k^2} \hat{\psi}_{\mathbf{k}} \hat{\psi}_{-\mathbf{k}} + \text{c.c.}\right] + \mathcal{O}(|\hat{\psi}_{\mathbf{k}}|^4), \tag{13c}$$

where $g(x) \equiv (x + e^{-x} - 1)/x$. The Zeeman energy takes the form

$$\mathcal{E}_{\rm z} = \beta \sum_{k} |\hat{\psi}_{\mathbf{k}}|^2, \tag{13d}$$

where $\beta = B/(4\pi M_s)$ is the dimensionless magnetic field in units of the saturation field. The anisotropy energy can be written as

$$\mathcal{E}_{\rm an} = \alpha \sum_k |\hat{\psi}_{\mathbf{k}}|^2 + \mathcal{O}(|\hat{\psi}_{\mathbf{k}}|^4), \tag{13e}$$

where $\alpha = K/(4\pi M_s^2)$ is the dimensionless anisotropy coefficient.

Details of the derivation of contributions 13b and 13c in the wave-vector space can be found in Appendix A of Ref. [9].

The current-action function $\mathcal{F}$ in the wave space has the simple form

$$\mathcal{F} = \frac{\varkappa}{2} \sum_{\mathbf{k}} |\hat{\psi}_{\mathbf{k}}|^2. \tag{14}$$

Substituting (13) and (14) in (11), we obtain the set of linear equations for the complex amplitudes $\hat{\psi}_{\mathbf{k}}$ and $\hat{\psi}^*_{-\mathbf{k}}$:

$$\begin{aligned} -i\dot{\hat{\psi}}_{\mathbf{k}} &= \left[k^2\ell^2 - 1 + \frac{g(hk)}{2} + b + i\frac{\varkappa}{2}\right]\hat{\psi}_{\mathbf{k}} + \\ &+ \frac{g(hk)}{2}\frac{(k^x + ik^y)^2}{k^2}\hat{\psi}^*_{-\mathbf{k}}, \\ i\dot{\hat{\psi}}^*_{-\mathbf{k}} &= \left[k^2\ell^2 - 1 + \frac{g(hk)}{2} + b - i\frac{\varkappa}{2}\right]\hat{\psi}^*_{-\mathbf{k}} + \\ &+ \frac{g(hk)}{2}\frac{(k^x - ik^y)^2}{k^2}\hat{\psi}_{\mathbf{k}}, \end{aligned} \tag{15}$$

where $b = \alpha + \beta$.

Looking for the solutions of Eq. (15) in the form

$$\hat{\psi}_{\mathbf{k}} = \Psi_+ e^{z(k)t}, \qquad \hat{\psi}^*_{-\mathbf{k}} = \Psi_- e^{z(k)t}, \tag{16}$$

where $\Psi_\pm$ are time independent amplitudes, we obtain the following condition for the rate constant $z(k)$:

$$z(k) = -\frac{\varkappa}{2} \pm \tilde{\varkappa}(k). \tag{17}$$

Here, the function $\tilde{\varkappa}(k)$ is given by

$$\tilde{\varkappa}(k) = \sqrt{(1 - k^2\ell^2 - b)\,(k^2\ell^2 + g(hk) - 1 + b)}. \tag{18a}$$

With regard for Eq. (17), we can conclude that if the function $\tilde{\varkappa}(k)$ is complex-valued, then the saturated state of the film is stable. If the value of the function $\tilde{\varkappa}(k)$ is real, then we have two different cases: for strong currents when $\varkappa > 2\tilde{\varkappa}$, we have $\mathrm{Re}\, z(k) < 0$. Therefore, the stationary state of the system is the saturated state with $m_z = 1$. However, for smaller currents $\varkappa < 2\tilde{\varkappa}$, the instability of the saturated state develops. The function $2\tilde{\varkappa}(k)$ for different values of the parameter b is shown in Fig. 2. One can see that $\tilde{\varkappa}(k)$ is a nonmonotonic function,

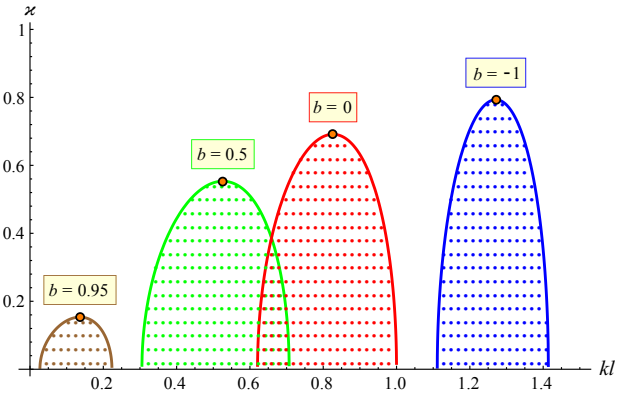

Fig. 2. (Color online) Influence of the parameter b on the instability domains (filled regions) of the transversally saturated permalloy ($\ell = 5.3$ nm) film with the thickness $h = 20$ nm. The instability domains are determined by condition (19). Points at the maxima determine the saturation current $\varkappa_s$ for the given b

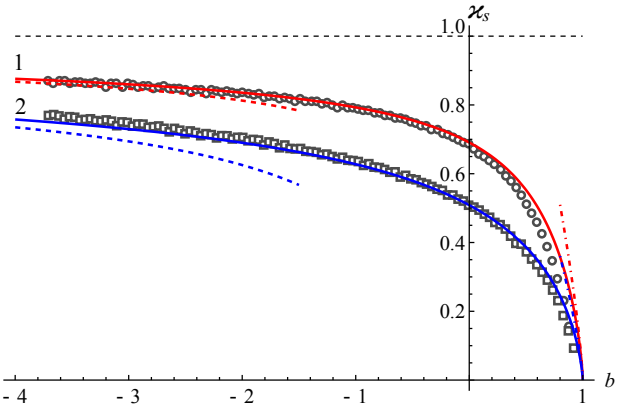

Fig. 3. (Color online) Dependence of the saturation current $\varkappa_s$ on the magnetic field. Solid line corresponds to the analytical solution obtained from (18) and the results of micromagnetic simulations (see the text) are shown by markers. Dashed lines correspond to asymptotic (20b) and dot-dashed lines show the asymptotics (20a). Dependences 1 and 2 correspond to different thicknesses: $h = 20$ nm and $h = 10$ nm, respectively

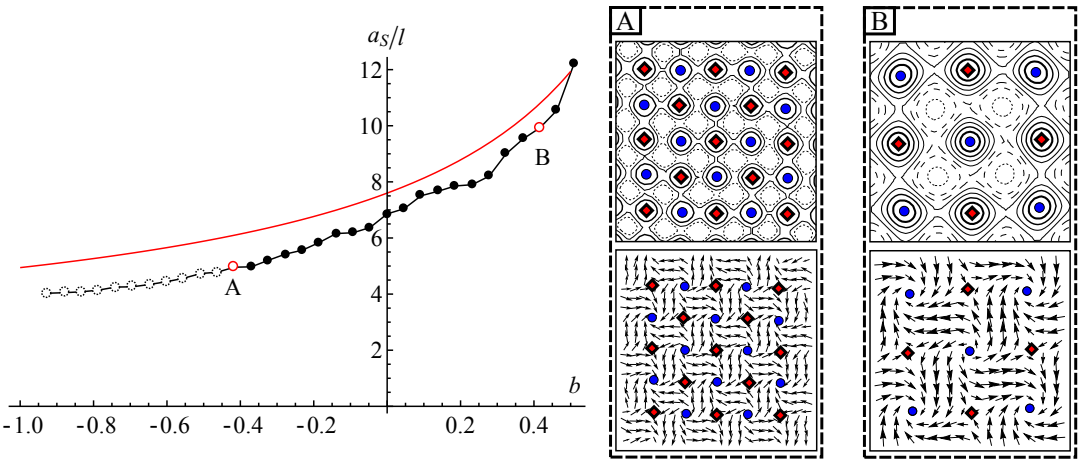

Fig. 4. (Color online) Dependence of the period of VAL, which appears in the pre-saturated regime, on the applied field. The data obtained using the micromagnetic modelling (see the text) are shown by markers, dark disks correspond to the VAL, whereas the dashed circles represents the fluid-like state of the vortex-antivortex system (see Ref. [8, 9]). The solid line corresponds to the dependence $2\pi/K_0$ obtained from (18b). The insets A and B show the magnetization distribution in VAL for the cases of negative and positive fields, respectively. The upper parts of the insets show the m_z-component distribution: with decreasing the value of m_z, the contour line becomes thinner. When m_z is close to the minimum value, the contours become dashed. The magnetization distribution within the film plane is shown by arrows in the bottom parts of the insets; disks and diamonds show the centers of vortices and antivortices, respectively. The size of the inset area is 50×50 nm. The data were obtained for the current density $J = 38 \times 10^{12}$ A/m^2

which reaches its maximum value $\tilde{\varkappa}_c$ at $k = K_0$:

$$\frac{\mathrm{d}\tilde{\varkappa}(k)}{\mathrm{d}k} = 0, \quad \tilde{\varkappa}_c = \max_k \tilde{\varkappa}(k) \equiv \tilde{\varkappa}(K_0). \tag{18b}$$

Thus, the value $\tilde{\varkappa}_c$ determines the lowest current, at which the saturated state remains stable, namely the saturation current:

$$\varkappa_s = 2\tilde{\varkappa}_c \Rightarrow J_s = 2\frac{J_0}{\eta}\tilde{\varkappa}_c. \tag{18c}$$

The instability domains, which are determined by condition

$$\tilde{\varkappa} \in \mathbb{R}, \quad \text{and} \quad \varkappa < \varkappa_s, \tag{19}$$

are shown in Fig. 2 as filled regions. Maximum values of the shown dependences determine the saturation current $\varkappa_s$ for the given value of the b-parameter. The dependence $\varkappa_s(b)$ is shown in Fig. 3

One can see that, for $b > 1$, the magnetic film is perpendicularly saturated without current. For example, this case can be realized for a magnetically soft film ($\alpha = 0$), when the external field exceeds the saturation value $\beta > 1$. The analysis of (18) enables us to obtain the following asymptotic behavior:

$$\varkappa_s \approx 2\sqrt{\frac{h}{\ell}}\left(\frac{1-b}{3}\right)^{3/4}, \quad b \lessapprox 1, \tag{20a}$$

$$\varkappa_s \approx 1 - \frac{\ell}{h\sqrt{|b|}}, \quad b \to -\infty. \tag{20b}$$

According to (20b), the saturation current is a quantity bounded from above: $\varkappa_s < 1$ for any values of parameters. This means that, for currents $\varkappa \geqslant 1$, the perpendicularly saturated magnetic film remains stable for any values of magnetic field and uniaxial anisotropy constant. In other words, if the current $\varkappa \geqslant 1$ is applied, then the magnetization reversal is not possible with a perpendicular magnetic field of any (even infinitely large) amplitude. We call this phenomenon "rigid saturation".

The critical current $\varkappa_c = 1$ has the dimensional form

$$J_c = \frac{4\pi M_s^2 |e| h}{\hbar\eta}. \tag{21}$$

Thus, the current J_c is determined only by material parameters (saturation magnetization) and the film thickness. For the case of a permalloy film with the thickness $h = 20$ nm and the rate of spin polarization $\eta = 0.4$, expression (21) yields $J_c = 70.6 \times 10^{12}$ A/m^2.

Thus, we determine the physical meaning of J_0 as the minimal current density, which provides the rigid saturation (for the case of the full spin-polarization $\eta = 1$).

To verify our analytical results, we used full-scale OOMMF [14] micromagnetic simulations. This modeling was performed with material parameters of permalloy as follows: the saturation magnetization $M_S = 8.6 \times 10^5$ A/m, and the exchange constant $A = 1.3\times\ \times 10^{-11}$ J/m. These values of parameters correspond to the exchange length $\ell = 5.3$ nm and the saturation field for an infinite film $B_s = = 1.081$ T. Since the external field and the anisotropy are included into the problem in equivalent ways, see Eqs. (13d), (5), (15), and (18a). In the simulations, we restrict ourselves only to the case with a magnetic field, neglecting the anisotropy ($\alpha = 0$). Not being able to simulate the unbounded film, we chose two nanodisks with the diameter $D = 350$ nm and the thicknesses $h = 20$ nm and $h = 10$ nm, and the mesh size was $3 \times 3 \times h$ nm. In the absence of a magnetic field and a current, the ground magnetic state of nanodisks of the mentioned sizes is related to the vortex distribution of the magnetization (see Fig. 1). To these nanodisks, we simultaneously apply an external magnetic field of the form $B(t) = B_0(1 - e^{-t/\Delta t})$ and the spin polarized current $J(t) = t\Delta J/\Delta t$, where $\Delta t = 1$ ns, $\Delta J = 10^{11}$ A/m^2 with the rate of spin polarization $\eta = 0.4$. The gradual increase of the field and the current allows us to avoid an intense magnon dynamics. The amplitude of the magnetic field was varied in the interval $B_0 \in [-4, 0.95]$ T with the step $\Delta B_0 = 0.05$ T. The current was increased until the saturation was achieved. As a criterion of saturation, we used the relation $M_z/M_s > 0.999999$, where M_z is the total magnetization along the $\hat{\mathbf{z}}$-axis. The resulting dependence $J_s(B)$ in the dimensionless form is shown in Fig. 3 by markers. Note a good agreement between the theoretical prediction and the numerical experiment. The reason for a slight discrepancy in the region $b \lessapprox 1$ is that the saturation field for a finite-size nanodisk B_s' is slightly smaller than B_s.1

It is known [8, 9] that the VAL usually appears in pre-saturated regime of the ferromagnetic film, see insets of Fig. 4. Here, we study numerically how the perpendicular magnetic field changes the properties of VAL. We obtained that the positive field (the field direction coincides with the current direction) increases the constant of VAL a_S, whereas the negative field (opposite to the current) decreases a_S. The resulting dependence $a_S(b)$ is presented in Fig. 4. As is seen, the lattice constant $a_S(b)$ is very close to the value $\bar{a}_S = 2\pi/K_0$, where K_0 is the wave vector of unstable magnons for the case $\varkappa \lessapprox \varkappa_s$, see (18b). Assuming that the mismatch between a_S and $\bar{a}_S$ remains small for all values of parameters, one can use (18) to obtain the following asymptotic behavior: $a_S \sim 1/(1-b)$ for $b \lessapprox 1$ and $a_S \sim 1/\sqrt{|b|}$ for $b \to -\infty$.

3. Conclusions

The perpendicular magnetic field drastically changes the process of saturation of magnetic films with spin-polarized current. It is shown that the saturation current J_s is decreased (increased) in the case of a codirected (oppositely directed) magnetic field and a current. There exists the critical current $J_c > J_s$, which provides the "rigid" saturation, namely the saturated state that is stable with respect to the transverse magnetic field of any amplitude and direction. The critical current J_c is determined only by material parameters (saturation magnetization) and the film thickness. The actions of a perpendicular magnetic field and a uniaxial anisotropy on the stability of the saturated state are equivalent. The magnetic field changes the constant of a vortex-antivortex lattice a_S, which appears in the pre-saturated regime: a_S infinitely increases if the field approaches the saturation value, and a_S decreases if the field is increased in the opposite direction. For large opposite fields, the fluid-like dynamics of a vortex-antivortex system is observed instead of the static vortex-antivortex lattice.

The authors are grateful to Yu.B. Gaididei and D.D. Sheka for the fruitful discussions. The present work was partially supported by the National Academy of Sciences of Ukraine (project No. 0110U007540).

1. J. Lindner, Superlattices and Microstructures **47**, 497 (2010).
2. S. Bohlens, B. Krüger, A. Drews, M. Bolte, G. Meier, and D. Pfannkuche, Appl. Phys. Lett. **93**, 142508 (pages 3) (2008).
3. A. Drews, B. Kruger, G. Meier, S. Bohlens, L. Bocklage, T. Matsuyama, and M. Bolte, Applied Physics Letters **94**, 062504 (pages 3) (2009).
4. A.D. Kent, B. Ozyilmaz, and E. del Barco, Appl. Phys. Lett. **84**, 3897 (2004).
5. J. C. Slonczewski, J. Magn. Magn. Mater. **159**, L1 (1996).
6. L. Berger, Phys. Rev. B **54**, 9353 (1996).
7. J.C. Slonczewski, J. Magn. Magn. Mater. **247**, 324 (2002).

8. O.M. Volkov, V.P. Kravchuk, D.D. Sheka, and Y. Gaididei, Phys. Rev. B **84**, 052404 (2011).
9. Y. Gaididei, O.M. Volkov, V.P. Kravchuk, and D. D. Sheka, Phys. Rev. B **86**, 144401 (2012).
10. A. Dussaux, B. Georges, J. Grollier, V. Cros, A. Khvalkovskiy, A. Fukushima, M. Konoto, H. Kubota, K. Yakushiji, S. Yuasa, et al., Nat Commun **1**, 1 (2010).
11. A. Dussaux, A. V. Khvalkovskiy, P. Bortolotti, J. Grollier, V. Cros, and A. Fert, Phys. Rev. B **86**, 014402 (2012).
12. V. Sluka, A. Kákay, A.M. Deac, D.E. Bürgler, R. Hertel, and C.M. Schneider, Journal of Physics D: Applied Physics **44**, 384002 (2011).
13. A.I. Akhiezer, V.G. Bar'yakhtar, and S.V. Peletminskiĭ, *Spin Waves* (North-Holland, Amsterdam, 1968).
14. *The Object Oriented MicroMagnetic Framework*, developed by M. J. Donahue and D. Porter mainly, from NIST. We used the 3D version of the 1.2α4 release, URL `http://math.nist.gov/oommf/`.

Received 18.04.13

О.М. Волков, В.П. Кравчук

НАСИЧЕННЯ МАГНІТНИХ ПЛІВОК СПІН-ПОЛЯРИЗОВАНИМ СТРУМОМ В ПРИСУТНОСТІ МАГНІТНОГО ПОЛЯ

Р е з ю м е

Теоретично досліджено вплив поперечного магнітного поля на процес насичення феромагнітної плівки під дією спін-поляризованого струму. Показано, що струм насичення J_s зменшується (збільшується) у випадку однаково (протилежно) напрямлених струму і магнітного поля. Існує критичний струм $J_c > J_s$, який забезпечує "жорстке" насичення – насичений стан є стійким по відношенню до зовнішнього магнітного поля з довільними амплітудою та напрямком. Чисельно досліджено вплив магнітного поля на вихор-антивихрові кристали, що виникають в режимі квазінасичення. Усі отримані аналітичні результати перевірені за допомогою мікромагнітних моделювань.